

Exendin-4–Based Radiopharmaceuticals for Glucagonlike Peptide-1 Receptor PET/CT and SPECT/CT

Damian Wild^{1,2}, Andreas Wicki³, Rosalba Mansi^{4,5}, Martin Béché^{5,6}, Boris Keil⁷, Peter Bernhardt⁸, Gerhard Christofori³, Peter J. Ell², and Helmut R. Mäcke^{4,5}

¹Clinic and Institute of Nuclear Medicine, University Hospital Basel, Basel, Switzerland; ²Institute of Nuclear Medicine, University College London, London, United Kingdom; ³Institute of Biochemistry and Genetics, Center for Biomedicine, University of Basel, Basel, Switzerland; ⁴Division of Radiological Chemistry, University Hospital Basel, Basel, Switzerland; ⁵Department of Nuclear Medicine, University Hospital Freiburg, Freiburg, Germany; ⁶Department of Nuclear Medicine, Hospital of the Philipps-University, Marburg, Germany; ⁷Department of Radiology, Hospital of the Philipps-University, Marburg, Germany; and ⁸Department of Radiation Physics, University of Gothenburg, Göteborg, Sweden

Strong overexpression of glucagonlike peptide-1 (GLP-1) receptors in human insulinoma provides an attractive target for imaging. The first clinical trials demonstrated that GLP-1 receptor SPECT/CT using [Lys⁴⁰(Ahx [6-aminohexanoic acid]-DOTA-¹¹¹In)NH₂]-exendin-4 can localize hardly detectable insulinomas. However, [Lys⁴⁰(Ahx-DOTA-¹¹¹In)NH₂]-exendin-4 imaging has drawbacks related to the use of ¹¹¹In in that it is costly and carries a relatively high radiation burden for the patient. The aim of this study was the preclinical evaluation of [Lys⁴⁰(Ahx-DOTA-⁶⁸Ga)NH₂]-exendin-4 for PET/CT and [Lys⁴⁰(Ahx-hydrazinonicotinamide [HYNIC]-^{99m}Tc)NH₂]-exendin-4 for SPECT/CT. **Methods:** Internalization, biodistribution, dosimetry, and imaging studies were performed in the Rip1Tag2 mouse model of pancreatic β -cell carcinogenesis and compared with our gold standard [Lys⁴⁰(Ahx-DOTA-¹¹¹In)NH₂]-exendin-4. Poly-glutamic acid and Gelofusine, a gelatin-based plasma expander, were used for renal uptake reduction studies. **Results:** The tumor uptake of [Lys⁴⁰(Ahx-DOTA-⁶⁸Ga)NH₂]-exendin-4 was 205 ± 59 percentage injected activity per gram of tissue at 4 h. Other GLP-1 receptor-positive organs showed more than 4.8 times lower radioactivity uptake. [Lys⁴⁰(Ahx-HYNIC-^{99m}Tc/ethylenediaminediacetic acid [EDDA])NH₂]-exendin-4, compared with its ¹¹¹In- and ⁶⁸Ga-labeled sister compounds, showed significantly less tumor and organ uptake. The significantly lower tumor and organ uptake of [Lys⁴⁰(Ahx-HYNIC-^{99m}Tc/EDDA)NH₂]-exendin-4 did not result in inferior tumor-to-organ ratios or reduced image quality. All radiolabeled peptides tested showed a high tumor-to-background ratio, resulting in the visualization of small tumors (maximum diameter between 1.0 and 3.2 mm) by SPECT and PET. The only exception was the kidneys, which also showed high uptake. This uptake could be reduced by 49%–78% using poly-glutamic acid, Gelofusine, or a combination of the 2. The estimated effective radiation dose was 3.7 μ Sv/MBq for [Lys⁴⁰(Ahx-HYNIC-^{99m}Tc/EDDA)NH₂]-exendin-4, which was 8 times less than that for [Lys⁴⁰(Ahx-DOTA-⁶⁸Ga)NH₂]-exendin-4 and 43 times less than

that for [Lys⁴⁰(Ahx-DOTA-¹¹¹In)NH₂]-exendin-4. **Conclusion:** These promising pharmacokinetic and imaging data show that [Lys⁴⁰(Ahx-DOTA-⁶⁸Ga)NH₂]-exendin-4 and [Lys⁴⁰(Ahx-HYNIC-^{99m}Tc/EDDA)NH₂]-exendin-4 are suitable candidates for clinical GLP-1 receptor imaging studies.

Key Words: glucagon-like peptide-1 receptor; insulinoma; exendin-4; ⁶⁸Ga; ^{99m}Tc

J Nucl Med 2010; 51:1059–1067
DOI: 10.2967/jnumed.110.074914

Over the last 15 y, peptide receptor targeting of cancer cells with radiolabeled peptides has become an important method for the diagnosis and treatment of cancer patients (1,2).

The high-density distribution of membrane peptide receptors in many different tumors, as shown on in vitro autoradiographic studies, represents the molecular basis of this application (1). [¹¹¹In-diethylenetriaminepentaacetic acid (DTPA)⁰]-octreotide (OctreoScan; Covidien) was the first probe for somatostatin receptor subtype 2 targeting to become an integral part of the routine diagnostic work-up of patients with gastroenteropancreatic neuroendocrine tumors (3). Especially in gut carcinoid tumors and gastrinomas, [¹¹¹In-DTPA⁰]-octreotide proved superior to conventional imaging methods such as sonography, CT, and MRI (4–6). In insulinomas, the sensitivity of [¹¹¹In-DTPA⁰]-octreotide is below 50% (7) because somatostatin receptor subtype 2 is expressed by less than 60% of insulinomas (8). The conventional imaging methods also have limited sensitivity because of the small size of insulinomas (9,10). The amine precursor 6-¹⁸F-fluoro-L-dopa shows controversial results, with sensitivities ranging from 17% up to 90% (11,12). Only angiography in combination with intraarterial calcium stimulation and

Received Jan. 16, 2010; revision accepted Mar. 11, 2010.
For correspondence or reprints contact: Helmut R. Mäcke, University Hospital Freiburg, Hugstetter Strasse 55, D-79106 Freiburg, Germany.
E-mail: helmut.maecke@uniklinik-freiburg.de
COPYRIGHT © 2010 by the Society of Nuclear Medicine, Inc.

venous sampling has been shown to improve the sensitivity, but this is an invasive procedure with a concomitant risk of complications (13). Thus, there is a clear need for a method that improves preoperative insulinoma imaging, especially in view of the fact that preoperative localization facilitates surgery for insulinoma, which is the only curative treatment option (10,14).

A promising new approach is the targeting of glucagon-like peptide-1 (GLP-1) receptors because their high densities in insulinoma provide an attractive target for imaging using GLP-1 receptor-avid radioligands. Especially in benign insulinoma, the GLP-1 receptor density is high, with almost 100% incidence (8). Consequently, GLP-1 receptor-avid radioligands have been developed and evaluated (15,16). Preclinical animal studies have shown the ability of [Lys⁴⁰(Ahx [6-aminohexanoic acid]-DTPA-¹¹¹In)NH₂]-exendin-4 to successfully localize small insulinomas in the Rip1Tag2 mouse tumor model (17). Treatment studies in the same animal tumor model have even shown the potential of GLP-1 receptor targeting as a therapeutic approach (18). Most important, the first trials in patients showed promising results in the noninvasive localization of insulinomas (19). In 6 of 6 patients, [Lys⁴⁰(Ahx-DOTA-¹¹¹In)NH₂]-exendin-4 SPECT/CT successfully detected pancreatic and ectopic insulinomas, which had previously not been identified with certainty using conventional methods (20). However, [Lys⁴⁰(Ahx-DOTA-¹¹¹In)NH₂]-exendin-4 has several drawbacks related to the use of ¹¹¹In, resulting in a relatively high radiation burden for the patient. A ^{99m}Tc-labeled GLP-1 receptor analog may overcome these drawbacks, and a PET tracer may have advantages over conventional GLP-1 receptor imaging with ¹¹¹In.

The aim of this study was the preclinical evaluation of [Lys⁴⁰(Ahx-DOTA-⁶⁸Ga)NH₂]-exendin-4 for PET/CT and [Lys⁴⁰(Ahx-hydrazinonicotinamide [HYNIC]-^{99m}Tc/ethylenediaminediacetic acid [EDDA])NH₂]-exendin-4 for SPECT/CT. Internalization, biodistribution, imaging, and dosimetry studies were performed and compared with our gold standard, [Lys⁴⁰(Ahx-DOTA-¹¹¹In)NH₂]-exendin-4. Most in vivo studies were performed in transgenic Rip1-Tag2 mice, which is an animal model suitable for in vivo GLP-1 receptor targeting (17).

MATERIALS AND METHODS

Abbreviations of the common amino acids are in accordance with the recommendations of the Commission of Biochemical Nomenclature of the International Union of Pure and Applied Chemistry–International Union of Biochemistry (21).

Reagents and Instrumentation

[Lys⁴⁰(Ahx-DOTA)NH₂]-exendin-4 and [Lys⁴⁰(Ahx-HYNIC)NH₂]-exendin-4 were custom-synthesized by Anawa Trading SA and Peptide Specialty Laboratories GmbH, respectively. Matrix-assisted laser desorption ionization–mass spectrometry measurements were done on a Voyager sSTR equipped with an Nd:YAG laser (355 nm) (Applied BioSystems). ⁶⁷GaCl₃, ¹¹¹InCl₃, and the ^{99m}Mo/^{99m}Tc generator were obtained from Covidien. The ⁶⁸Ge/⁶⁸Ga

generator was delivered by Eckert and Ziegler. Analytic reversed-phase high-performance liquid chromatography (HPLC) was performed on a Bischof HPLC system (Metrohm AG) with HPLC pumps (model 2250) and a λ-1010 ultraviolet detector (Metrohm AG), as described elsewhere (17).

Dulbecco's modified Eagle's medium (high glucose, pH 7.4) supplemented with 10% fetal bovine serum, 2% L-glutamine, and 1% penicillin–streptomycin from Gibco BRL was used. C57BL/6J mice and transgenic Rip1Tag2 mice were scanned and analyzed either with an inline PET/CT system (Discovery STE; GE Healthcare) or with an MRI scanner (Magnetom Expert; Siemens) and a SPECT scanner (e.cam SPECT scanner; Siemens), which was modified with a multipinhole aperture (22). SPECT images were reconstructed using a HiSPECT reconstruction program (SciVis). SPECT and MR images were manually fused on a Hermes workstation (Hermes Medical Solutions). All dosimetric calculations were performed using the OLINDA/EXM 1.0 software (Vanderbilt University, 2003) (23).

Radiolabeling of Peptides

[Lys⁴⁰(Ahx-DOTA)NH₂]-exendin-4 with ¹¹¹InCl₃ was radiolabeled as previously described (17). The radiolabeled solution was then subjected to quality control by analytic reversed-phase HPLC.

[Lys⁴⁰(Ahx-DOTA)NH₂]-exendin-4 was radiolabeled with ⁶⁷Ga as described for ¹¹¹InCl₃. An aliquot of 40 μL (0.2 mmol/L, 40 μg) of peptide was dissolved in 200 μL of sodium acetate buffer (0.4 mol/L, pH 5.0) before 23 MBq of ⁶⁷GaCl₃ were added.

⁶⁸Ga was eluted from a commercially available generator according to the method of Zhernosekov et al. (24). Afterward, the eluate was purified of ⁶⁸Ge(IV), Zn(II), Ti(IV), and Fe(III) using a 50W-X8 cation exchanger chromatographic column (Bio-Rad) (<400 mesh) and 80% acetone/0.15N hydrochloric acid. After elution from the exchanger column (400 μL of 97.6% acetone/0.05N HCl solution), ⁶⁸Ga(III) was incubated with 50 μg of [Lys⁴⁰(Ahx-DOTA)NH₂]-exendin-4 in a 0.25 M N-(2-hydroxyethyl)piperazine-N'-(2-ethanesulfonic acid) solution (400 μL; pH 3.6–3.9) for 5 min at 95°C using a microwave oven (Biotage).

The radiolabeling of [Lys⁴⁰(Ahx-HYNIC)NH₂]-exendin-4 with ^{99m}Tc followed a 2-vial kit formulation. One milliliter of a solution containing 15 mg (84 μmol) of tricine, 35 μg of [Lys⁴⁰(Ahx-HYNIC)NH₂]-exendin-4, and 40 μg of SnCl₂ (10 μL of 22.2 mM SnCl₂·2 H₂O in 0.1 M HCl) was filtered into a glass vial strictly under air protection. One-half milliliter of a solution containing 5 mg of EDDA (pH was adjusted to 7 with 1 M NaOH) was filtered into a second glass vial. The glass vials were immediately frozen in liquid nitrogen, lyophilized, and closed afterward under a vacuum. For labeling, the EDDA vial was reconstituted with 0.5 mL of saline and added to the [Lys⁴⁰(Ahx-HYNIC)NH₂]-exendin-4 vial, followed by 370 MBq of ^{99m}TcO₄⁻, and incubated for 10 min at 95°C. After cooling to room temperature, the reaction mixture was analyzed by HPLC.

Cell Culture, Radioligand Internalization, and Externalization Studies

GLP-1 receptor-expressing β-tumor cells were established from β-cell tumors of Rip1Tag2 mice, as described previously (17). For internalization experiments, the cells were seeded at a density of 0.8–1 million cells per well in 6-well plates and incubated overnight with internalization buffer. Afterward, 0.25 pmol of the respective radiopeptide was added to the medium

(final concentration, 0.17 nmol/L) and incubated at 37°C. To determine nonspecific membrane binding and internalization, a large excess of unlabeled peptide was used in selected wells. The internalization was stopped at appropriate time points (30 min and 1, 2, and 4 h) by removing the medium, and the cells were treated as described previously (17).

For externalization studies, β -tumor cells (0.8–1 million) were incubated with 0.25 pmol of radiopeptide (0.17 nmol/L) for 120 min. Then the medium was removed, and the cells were treated as described previously (17). All in vitro experiments were performed twice (triplicates in each experiment).

Animal Model

Animals were maintained and treated in compliance with the guidelines of the Swiss regulations (approval 789). Male and female Rip1Tag2 transgenic mice and female wild-type mice (C57BL/6J mice) were used for biodistribution studies, pinhole SPECT/MRI, and PET/CT. Transgenic Rip1Tag2 mice developed β -cell tumors in the pancreas in a multistage tumorigenesis pathway. These tumors were characterized by a high expression of GLP-1 receptors (17). Phenotypic and genotypic analyses of Rip1Tag2 mice have been described previously (25). At intervention, all mice were between 11 and 13 wk old.

Biodistribution in Rip1Tag2 Mice

Ten picomoles (70–110 kBq) of the respective radiopeptide diluted in 100 μ L of a 1% human albumin solution were injected into the tail vein of Rip1Tag2 mice. Rip1Tag2 mice were sacrificed at the following time points after injection ($n = 3$ –6 per time point): For [Lys⁴⁰(Ahx-DOTA-¹¹¹In)NH₂]-exendin-4, mice were sacrificed at 1, 4, 12, 36, 84, and 168 h; for [Lys⁴⁰(Ahx-DOTA-⁶⁸Ga)NH₂]-exendin-4, at 0.5, 1, 2, and 4 h; and for [Lys⁴⁰(Ahx-HYNIC-^{99m}Tc/EDDA)NH₂]-exendin-4, at 0.5, 2, 4, and 18 h. Organs, blood, and tumors were collected, and the radioactivity was measured in a γ -counter. The radioactivity uptake in organs and tumors was calculated as percentage of injected activity per gram of tissue (%IA/g) and percentage of injected activity per organ (%IA/organ).

To determine the nonspecific uptake of the respective radiopeptide, Rip1Tag2 mice were coinjected with 10 pmol of the radiolabeled peptide and 5 nmol of the respective nonlabeled peptide and sacrificed 4 h later.

Radiation Dose Calculation

Mice biodistribution data were used to generate the residence time for each radiopeptide. Because of the absence of specific activity accumulation in bones and red marrow (18), a linear relationship between the blood residence time and red marrow residence time was assumed to estimate the red marrow radiation

dose (26). The proportionality factor was the ratio between the red marrow mass and the blood mass in humans.

OLINDA/EXM was used to integrate the fitted time–activity curves. Organ and effective doses were estimated with OLINDA/EXM using the whole-body adult female model and the weighting factors recommended by the International Commission on Radiological Protection (27). For all calculations, the assumption was made that the Rip1Tag2 mouse biodistribution, determined as the %IA/organ, was the same as the human biodistribution.

GLP-1 Receptor Imaging with Multipinhole SPECT/MRI

Two Rip1Tag2 mice were injected with 37 MBq of [Lys⁴⁰(Ahx-HYNIC-^{99m}Tc/EDDA)NH₂]-exendin-4 into the tail vein. Four hours after injection, multipinhole SPECT images of both Rip1Tag2 mice (under isoflurane anesthesia and lying prone) were obtained (22). Images were acquired from 60 angles, with a minimum of 30 kilo counts per angle, resulting in a scan time of 60 min. Shortly thereafter, Rip1Tag2 mice were scanned in an MRI scanner in the same position. To enhance the signal-to-noise ratio, a specially designed and modified small-animal saddle coil was used. Coronal high-resolution slices were obtained using a 3-dimensional (3D) double-echo-in-steady-state sequence. Transverse slices were reconstructed from the 3D dataset to obtain slices for image fusion. Reconstructed transverse MR and SPECT images were manually fused using the anatomic information obtained from both imaging modalities. After imaging, necropsy was performed in both animals, and the size of tumors was measured.

GLP-1 Receptor Imaging with PET/CT

One Rip1Tag2 mouse was injected with 10 pmol (130 kBq) of [Lys⁴⁰(Ahx-DOTA-⁶⁸Ga)NH₂]-exendin-4 as described above. Sixty minutes after injection, the mouse was sacrificed and bilateral nephrectomy was performed. PET images (3D mode) of the mouse lying prone were obtained for 1 h with a PET/CT hybrid scanner. The image matrix was 256 \times 256, and images were reconstructed as 1-mm-thick sections using an iterative algorithm. The CT data from the PET/CT examination were reconstructed in the transverse plane as 1-mm-thick sections. The following parameters were used for imaging: 130 kV, 80 mAs, 1.5 s per rotation, and 1 mm/s table speed.

Renal Uptake Reduction Studies

For renal uptake reduction studies, 80 mg (3–15 kD) of L-polyglutamic acid (PGA; Sigma-Aldrich) per milliliter or 40 mg of Gelofusine (Braun) per milliliter were dissolved in saline as described previously (28). Rip1Tag2 mice were injected intravenously with 100 μ L of one solution or 200 μ L of both solutions just before intravenous administration of 10 pmol of

TABLE 1. Comparison of Internalization Kinetics for ¹¹¹In-, ⁶⁷Ga-, and ^{99m}Tc-Labeled Exendin-4 in β -Tumor Cells

Compound	0.5 h	1 h	2 h	4 h
[Lys ⁴⁰ (Ahx-DOTA- ¹¹¹ In)NH ₂]-exendin-4	1.03 \pm 0.14	2.03 \pm 0.18	4.97 \pm 0.4	9.75 \pm 0.65
[Lys ⁴⁰ (Ahx-DOTA- ⁶⁷ Ga)NH ₂]-exendin-4	1.22 \pm 0.08	2.48 \pm 0.29	5.10 \pm 0.26	10.35 \pm 0.43
[Lys ⁴⁰ (Ahx-HYNIC- ^{99m} Tc/EDDA)NH ₂]-exendin-4	0.73 \pm 0.29	1.50 \pm 0.49	3.37 \pm 1.27	6.50 \pm 1.94
1-way ANOVA	$P = 0.002$	$P = 0.001$	$P = 0.003$	$P = 0.0001$

Values and SD are result of 2 independent experiments (triplicates in each experiment) and are expressed as specific internalization (% added radioactivity/10⁶ cells \pm SD). Significance was analyzed by 1-way ANOVA.

TABLE 2. Biodistribution in Rip1Tag2 Mice at 0.5, 1, 2, and 4 Hours After Injection of [Lys⁴⁰(Ahx-DOTA-⁶⁸Ga)NH₂]-Exendin-4

Organ	0.5 h	1 h	2 h	4 h
Lungs*	40.8 ± 3.5	42.5 ± 5.1	31.4 ± 2.9	42.5 ± 5.1
Pancreas*	17.0 ± 2.4	13.5 ± 4.4	16.8 ± 6.3	13.5 ± 1.0
Stomach*	4.05 ± 0.33	4.08 ± 0.59	2.56 ± 0.35	2.14 ± 0.77
Tumor*	185 ± 33	209 ± 44	207 ± 60	205 ± 59
Kidneys	255 ± 14	230 ± 33	252 ± 24	202 ± 34
Liver	0.88 ± 0.04	0.61 ± 0.11	0.63 ± 0.12	0.61 ± 0.11
Spleen	2.14 ± 0.12	1.91 ± 0.50	2.10 ± 0.73	2.28 ± 0.59
Muscle	1.30 ± 0.10	1.13 ± 0.51	0.97 ± 0.09	1.00 ± 1.03
Bone	1.03 ± 0.33	1.01 ± 0.91	1.07 ± 0.13	0.89 ± 0.52
Blood	2.08 ± 0.49	1.35 ± 0.17	0.49 ± 0.03	0.29 ± 0.10
Tumor/blood	88.9	155	423	706
Tumor/muscle	142	185	214	205
Tumor/pancreas	10.9	15.5	12.4	15.2
Tumor/lungs	4.52	4.91	6.60	4.82
Tumor/kidneys	0.72	0.91	0.82	1.01

*GLP-1 receptor-positive organs.
Results are expressed as %IA/g (mean ± SD), *n* ≥ 3.

[Lys⁴⁰(Ahx-DOTA-⁶⁸Ga)NH₂]-exendin-4. One hour later, Rip1-Tag2 mice (*n* = 3 per cohort) were sacrificed. One control animal and 1 PGA plus Gelofusine-treated animal underwent PET/CT just before tumor and organ collection. Finally, the radioactivity uptake in organs and tumors was calculated as %IA/g and %IA/organ.

Statistical Analysis

The calculation of means and SDs for internalization and biodistribution was performed in Excel (Microsoft). Correlation between the rate of internalization and tumor or lung uptake was analyzed in Microsoft Excel using linear regression analysis. Graphing and curve fitting were performed using Microcal Origin. One-way ANOVA for groups, including Tukey's posttest for pairwise comparison, was performed on Paleontological Statistics software. *P* values less than 0.05 were considered significant.

RESULTS

Synthesis and Radiolabeling

DOTA and HYNIC were coupled via the Lys side chain of the C-terminally extended exendin-4 using Ahx as a spacer. The composition and structural identity of [Lys⁴⁰(Ahx-DOTA)NH₂]-exendin-4 and [Lys⁴⁰(Ahx-HYNIC)NH₂]-exendin-4 were verified by analytic HPLC and matrix-assisted laser desorption ionization-mass spectrometry ([Lys⁴⁰(Ahx-DOTA)NH₂]-exendin-4: 4,815.21 [M⁺H⁺] and [Lys⁴⁰(Ahx-HYNIC)NH₂]-exendin-4: 4,563.78 [M⁺H⁺]). The labeling yield of [Lys⁴⁰(Ahx-DOTA-¹¹¹In)NH₂]-exendin-4 and [Lys⁴⁰(Ahx-HYNIC-^{99m}Tc/EDDA)NH₂]-exendin-4 was 98% and 95% at a specific activity of 19 GBq/μmol and 48 GBq/μmol, respectively. [Lys⁴⁰(Ahx-DOTA-⁶⁸Ga)NH₂]-

TABLE 3. Biodistribution in Rip1Tag2 Mice at 0.5, 2, 4, and 18 Hours After Injection of [Lys⁴⁰(Ahx-HYNIC-^{99m}Tc/EDDA)NH₂]-Exendin-4

Organ	0.5 h	2 h	4 h	18 h
Lungs*	14.6 ± 4.3	18.5 ± 5.9	15.9 ± 5.6	8.7 ± 1.9
Pancreas*	7.1 ± 2.0	9.6 ± 1.5	7.4 ± 2.2	6.0 ± 1.4
Stomach*	1.18 ± 0.32	1.36 ± 0.32	1.20 ± 0.30	1.05 ± 0.27
Tumor*	67 ± 13	98 ± 19	93 ± 20	50 ± 9
Kidneys	63 ± 10	57 ± 14	60 ± 12	42 ± 12
Liver	0.83 ± 0.20	0.71 ± 0.28	0.72 ± 0.20	0.74 ± 0.19
Spleen	0.59 ± 0.10	0.47 ± 0.17	0.52 ± 0.10	0.58 ± 0.10
Muscle	0.16 ± 0.08	0.13 ± 0.10	0.17 ± 0.08	0.09 ± 0.05
Bone	0.19 ± 0.03	0.16 ± 0.03	0.18 ± 0.03	0.21 ± 0.02
Blood	2.34 ± 0.47	0.55 ± 0.11	0.35 ± 0.13	0.19 ± 0.12
Tumor/blood	29	177	266	262
Tumor/muscle	419	754	547	556
Tumor/pancreas	9.5	10.2	12.6	8.4
Tumor/lungs	4.59	5.29	5.86	10.6
Tumor/kidneys	1.06	1.72	1.55	1.18

*GLP-1 receptor-positive organs.
Results are expressed as %IA/g (mean ± SD), *n* ≥ 3.

TABLE 4. Biodistribution Data and Tissue Radioactivity Ratios at 4 Hours After Injection of Respective Radiopeptide

Organs	Study parameter*	[Lys ⁴⁰ (Ahx-DOTA- ¹¹¹ In)NH ₂]-exendin-4	[Lys ⁴⁰ (Ahx-DOTA- ⁶⁸ Ga)NH ₂]-exendin-4	[Lys ⁴⁰ (Ahx-HYNIC- ^{99m} Tc/EDDA)NH ₂]-exendin-4	<i>P</i> (1-way ANOVA)
Lungs [†]	Nonblocked	39.7 ± 6.8	42.5 ± 5.1	15.9 ± 5.6	<0.0001
	Blocked	0.57 ± 0.01	0.90 ± 0.25	0.65 ± 0.17	
Pancreas [†]	Nonblocked	17.8 ± 3.9	13.5 ± 1.0	7.4 ± 2.2	<0.0001
	Blocked	0.90 ± 0.26	0.79 ± 0.27	0.34 ± 0.16	
Stomach [†]	Nonblocked	3.31 ± 0.86	2.14 ± 0.77	1.20 ± 0.30	<0.0001
	Blocked	0.60 ± 0.02	1.22 ± 0.40	0.35 ± 0.07	
Tumor [†]	Nonblocked	213 ± 75	205 ± 59	93.1 ± 19.9	<0.0001
	Blocked	9.35 ± 4.18	5.62 ± 3.85	5.45 ± 0.43	
Kidney	Nonblocked	243 ± 17	202 ± 34	60 ± 12	<0.0001
	Blocked	257 ± 30	193 ± 81	48 ± 7	
Liver	Nonblocked	1.03 ± 0.12	0.61 ± 0.11	0.72 ± 0.2	<0.0001
	Blocked	0.85 ± 0.18	0.51 ± 0.28	0.54 ± 0.21	
Spleen	Nonblocked	2.17 ± 0.54	2.28 ± 0.59	0.52 ± 0.1	<0.0001
	Blocked	1.77 ± 0.58	1.37 ± 0.47	0.37 ± 0.14	
Muscle	Nonblocked	1.23 ± 0.76	1.00 ± 1.03	0.17 ± 0.08	0.008
	Blocked	0.78 ± 0.32	0.82 ± 0.10	0.08 ± 0.03	
Bone	Nonblocked	0.36 ± 0.20	0.89 ± 0.52	0.18 ± 0.03	0.01
	Blocked	0.13 ± 0.03	0.46 ± 0.26	0.16 ± 0.09	
Blood	Nonblocked	0.26 ± 0.08	0.29 ± 0.10	0.35 ± 0.13	0.69
	Blocked	0.24 ± 0.03	0.39 ± 0.25	0.50 ± 0.29	
Tumor/blood		820	706	266	
Tumor/muscle		173	205	547	
Tumor/pancreas		12.0	15.2	12.6	
Tumor/lungs		5.37	4.82	5.86	
Tumor/kidneys		0.88	1.01	1.55	

*Blocked studies were blocked with 5 nmol of respective peptide.
[†]GLP-1 receptor-positive organs.
 Data are expressed as IA%/g (mean ± SD), *n* = 6; blockage study, *n* = 3.

exendin-4 was radiolabeled using microwave heating with a labeling yield of greater than 98% at a specific activity of 13 GBq/μmol.

In Vitro Internalization and Externalization Studies

Table 1 shows the results of specific internalization of GLP-1 receptor agonists into β-tumor cells. Between 80% and 99% of totally internalized radioligands were specifically internalized. The rate of internalization was not significantly different between the ¹¹¹In- and the ⁶⁷Ga-labeled exendin-4. A significant difference was found between ^{99m}Tc- and ¹¹¹In- and between ^{99m}Tc- and ⁶⁷Ga-labeled exendin-4.

The kinetics of externalization were studied with β-tumor cells exposed to the radiopeptide for 2 h at 37°C. Within 4 h, only 18.7%–23% of the radioligands were released from the β-tumor cells and the externalization leveled off (not shown). There was no significant difference in the rate of externalization among the 3 radiopeptides.

Animal Biodistribution Studies

We have shown previously that the tumor uptake of [Lys⁴⁰(Ahx-DTPA-¹¹¹In)NH₂]-exendin-4 is peptide amount-dependent, with the highest uptake at a peptide mass of

10 pmol (18). As a result, 10 pmol of radiopeptide was used in all biodistribution experiments. Biodistribution data and tumor-to-tissue ratios of [Lys⁴⁰(Ahx-DOTA-⁶⁸Ga)NH₂]-exendin-4 and [Lys⁴⁰(Ahx-HYNIC-^{99m}Tc/EDDA)NH₂]-exendin-4 are summarized in Tables 2 and 3, respectively. Both radiopeptides showed a fast blood clearance and high tumor-to-normal organ ratios already at early time points (Tables 2 and 3). One-way ANOVA showed significant differences among exendin-4 analogs (Table 4). [Lys⁴⁰(Ahx-HYNIC-^{99m}Tc/EDDA)NH₂]-exendin-4 showed the lowest and [Lys⁴⁰(Ahx-DOTA-¹¹¹In)NH₂]-exendin-4 the highest tumor and organ uptake. Tukey's posttest for individual comparison showed no difference in tumor uptake between [Lys⁴⁰(Ahx-DOTA-¹¹¹In)NH₂]-exendin-4 and [Lys⁴⁰(Ahx-DOTA-⁶⁸Ga)NH₂]-exendin-4. The accumulated activity in GLP-1 receptor-expressing organs such as lung and pancreas was high, at 42.5 ± 5.1 %IA/g and 13.5 ± 1.0 %IA/g 4 h after injection of [Lys⁴⁰(Ahx-DOTA-⁶⁸Ga)NH₂]-exendin-4. The highest uptake was found in the tumor and kidneys at 4 h after injection of the ¹¹¹In- and ⁶⁸Ga-labeled DOTA conjugate. Blocking with a 500-times excess of the respective cold ligand reduced the tumor uptake of all tested radiopeptides by more than 94%, whereas the kidney uptake was not affected.

TABLE 5. Radiation Dose Estimation Extrapolated to Humans After Injection of ^{111}In -, ^{68}Ga -, and $^{99\text{m}}\text{Tc}$ -Labeled Exendin-4

Organ/tissue	[Lys ⁴⁰ (Ahx-DOTA- ¹¹¹ In)NH ₂]-exendin-4	[Lys ⁴⁰ (Ahx-DOTA- ⁶⁸ Ga)NH ₂]-exendin-4	[Lys ⁴⁰ (Ahx-HYNIC- ^{99m} Tc/EDDA)NH ₂]-exendin-4
Adrenals	0.43	0.050	0.0079
Brain	0.064	0.014	0.0014
Breasts	0.064	0.015	0.0015
Gallbladder wall	0.26	0.029	0.0057
Gastrointestinal	0.14	0.020	0.0032
Lower large intestine wall			
Small intestine	0.32	0.068	0.0097
Stomach wall	0.20	0.029	0.0046
Upper large intestine wall	0.23	0.026	0.0055
Heart wall	0.10	0.01	0.0025
Kidneys	4.48	1.85	0.083
Liver	0.20	0.020	0.0046
Lungs	0.13	0.044	0.0046
Muscle	0.12	0.019	0.0024
Ovaries	0.16	0.021	0.0039
Pancreas	0.70	0.20	0.020
Red marrow	0.14	0.020	0.0030
Osteogenic cells	0.23	0.028	0.0060
Skin	0.064	0.015	0.0013
Spleen	0.37	0.035	0.068
Thymus	0.086	0.017	0.0020
Thyroid	0.069	0.015	0.0015
Urinary bladder wall	0.11	0.017	0.0026
Uterus	0.15	0.021	0.0036
Total body	0.14	0.029	0.0031
Effective dose (mSv/MBq)	0.155	0.0317	0.00372

Results are expressed as mean absorbed dose (mGy/MBq).

An important value for the diagnostic use of GLP-1 receptor tracers is the tumor-to-pancreas ratio, which was between 12 and 15.2 for all radiopeptides tested.

Dosimetry

Table 5 shows the radiation dose estimation extrapolated to humans after injection of [Lys⁴⁰(Ahx-DOTA-¹¹¹In)NH₂]-exendin-4, [Lys⁴⁰(Ahx-DOTA-⁶⁸Ga)NH₂]-exendin-4, and [Lys⁴⁰(Ahx-HYNIC-^{99m}Tc/EDDA)NH₂]-exendin-4. Bio-distribution data expressed as %IA/organ (Supplemental Tables 1–3; supplemental materials are available online only at <http://jnm.snmjournals.org>) were used to generate the residence time for each radiopeptide. The estimated effective radiation dose is 0.16 mSv/MBq for [Lys⁴⁰(Ahx-DOTA-¹¹¹In)NH₂]-exendin-4, 0.032 mSv/MBq for [Lys⁴⁰(Ahx-DOTA-⁶⁸Ga)NH₂]-exendin-4, and only 0.0037 mSv/MBq for [Lys⁴⁰(Ahx-HYNIC-^{99m}Tc/EDDA)NH₂]-exendin-4. The highest radiation dose was calculated for the kidneys.

In Vivo GLP-1 Receptor Imaging

Figure 1 shows the iteratively reconstructed multipinhole SPECT/MR images of 1 Rip1Tag2 mouse at 4 h after injection of 37 MBq of [Lys⁴⁰(Ahx-HYNIC-^{99m}Tc/EDDA)NH₂]-exendin-4. In contrast to high-resolution MRI, pinhole [Lys⁴⁰(Ahx-HYNIC-^{99m}Tc/EDDA)NH₂]-exendin-4

SPECT visualized 4 small insulinomas with a diameter between 1.0 and 3.2 mm. Other GLP-1 receptor-positive organs, such as the lung and pancreas, were hardly visible.

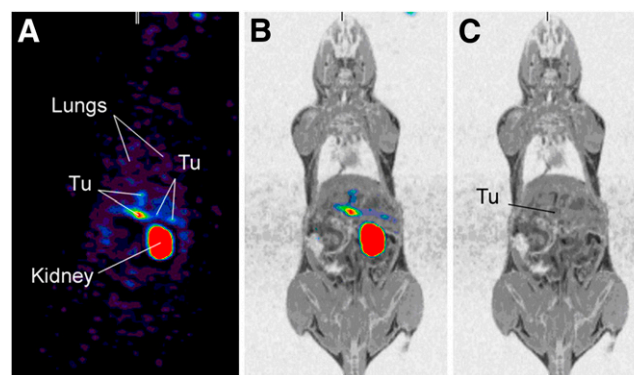


FIGURE 1. GLP-1 receptor SPECT/MRI of tumor-bearing Rip1Tag2 mouse at 4 h after injection of 37 MBq of [Lys⁴⁰(Ahx-HYNIC-^{99m}Tc/EDDA)NH₂]-exendin-4. Only multipinhole SPECT images (A) and corresponding multipinhole SPECT/MR fused images (B) show 4 tumor lesions (Tu) in pancreas with diameter between 1 and 3.2 mm. Corresponding MR images (C) show only largest tumor. There is intense tracer accumulation in kidneys but only weak uptake of [Lys⁴⁰(Ahx-HYNIC-^{99m}Tc/EDDA)NH₂]-exendin-4 in both lungs (A).

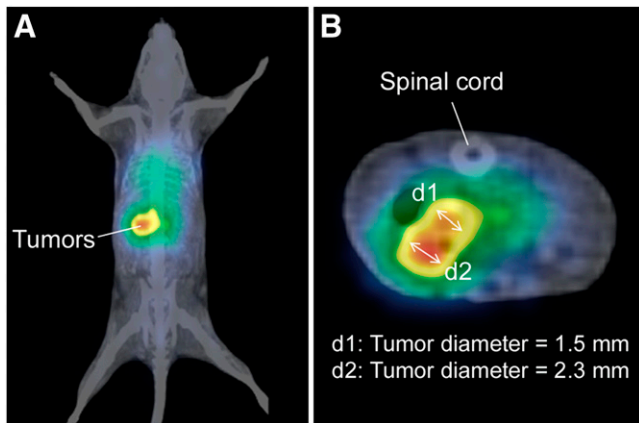


FIGURE 2. [$\text{Lys}^{40}(\text{Ahx-DOTA-}^{68}\text{Ga})\text{NH}_2$]-exendin-4 PET/CT of 1 Rip1Tag2 mouse after bilateral nephrectomy. Coronal (A) and transverse (B) PET/CT images show intense [$\text{Lys}^{40}(\text{Ahx-DOTA-}^{68}\text{Ga})\text{NH}_2$]-exendin-4 uptake in 2 tumor lesions with maximum diameter of 1.5 mm (d1) and 2.3 mm (d2), respectively. The coregistered CT scan was unremarkable at same location. There is no relevant uptake of [$\text{Lys}^{40}(\text{Ahx-DOTA-}^{68}\text{Ga})\text{NH}_2$]-exendin-4 elsewhere.

Figure 2 shows PET/CT images of 1 Rip1Tag2 mouse at 1 h after injection of 130 kBq of [$\text{Lys}^{40}(\text{Ahx-DOTA-}^{68}\text{Ga})\text{NH}_2$]-exendin-4. Before imaging, bilateral nephrec-

tomy was performed because tumor delineation from the kidneys was not possible before nephrectomy. After nephrectomy, PET/CT images demonstrated impressive focal uptake in 2 tumors in the pancreatic body after injection of only 130 kBq of [$\text{Lys}^{40}(\text{Ahx-DOTA-}^{68}\text{Ga})\text{NH}_2$]-exendin-4 (Figs. 2C and 2D). The maximal diameter of these tumors was only 2.3 and 1.5 mm.

Renal Uptake Reduction Studies

Figures 3A and 3B show kidney and tumor uptake of [$\text{Lys}^{40}(\text{Ahx-DOTA-}^{68}\text{Ga})\text{NH}_2$]-exendin-4 after pretreatment with PGA or Gelofusine. The uptake in tissues other than kidneys did not differ significantly between the control group and the kidney protection group. In comparison with the control group, PGA and Gelofusine showed a kidney uptake reduction of 49% and 60%, respectively ($P < 0.01$). The combination of PGA and Gelofusine was even more effective than PGA alone, with a kidney uptake reduction of 78% ($P = 0.0002$). The tumor-to-kidney ratio was 4.9 after PGA plus Gelofusine treatment and 2.4 after Gelofusine treatment. However, no significant difference in kidney protection was found between Gelofusine alone and the combination of PGA and Gelofusine ($P = 0.055$). Figures 3C and 3D show [$\text{Lys}^{40}(\text{Ahx-DOTA-}^{68}\text{Ga})\text{NH}_2$]-exendin-4 PET/CT scans of 1 animal with kidney protection and 1 animal without kidney protection.

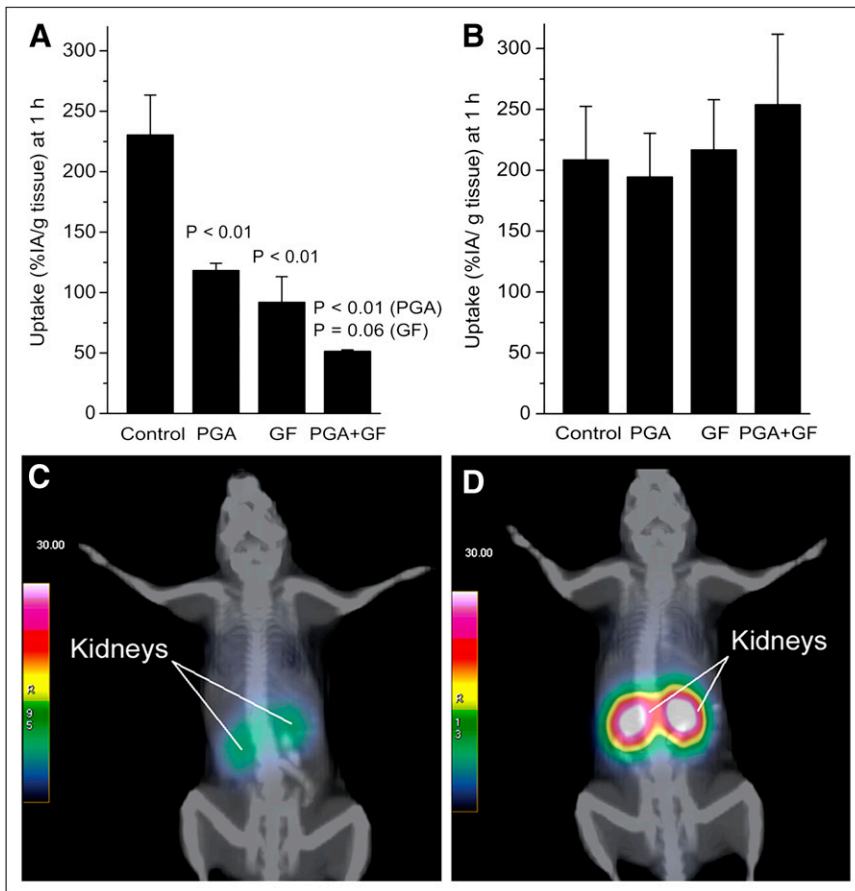


FIGURE 3. Biodistribution and PET/CT of Rip1Tag2 mice 1 h after injection of [$\text{Lys}^{40}(\text{Ahx-DOTA-}^{68}\text{Ga})\text{NH}_2$]-exendin-4. PGA, Gelofusine, and combination of the 2 significantly reduce renal accumulation of [$\text{Lys}^{40}(\text{Ahx-DOTA-}^{68}\text{Ga})\text{NH}_2$]-exendin-4 (A). At same time, tumor uptake is not affected by PGA or Gelofusine (B). Combination of PGA and Gelofusine is more efficient than PGA and Gelofusine alone. PGA plus Gelofusine pretreated Rip1Tag2 mouse (C) shows 78% lower kidney uptake than untreated control (D). In both animals, distinct differentiation between tumors and kidneys was not possible.

DISCUSSION

GLP-1 receptor imaging is a novel approach for preoperative localization of insulinoma. First clinical studies using ^{111}In -labeled GLP-1 receptor agonist $[\text{Lys}^{40}(\text{Ahx-DOTA-}^{111}\text{In})\text{NH}_2]$ -exendin-4 detected 6 of 6 benign insulinomas (20). The present study describes new ^{68}Ga - and $^{99\text{m}}\text{Tc}$ -labeled GLP-1 receptor agonists for PET/CT and SPECT/CT, respectively. The pharmacokinetics of the new compounds were compared with our gold standard $[\text{Lys}^{40}(\text{Ahx-DOTA-}^{111}\text{In})\text{NH}_2]$ -exendin-4.

$[\text{Lys}^{40}(\text{Ahx-DOTA-}^{68}\text{Ga})\text{NH}_2]$ -exendin-4 showed not only a fast, high, and specific uptake in the tumors but also a high tumor-to-background ratio. The high kidney uptake was significantly reduced by the administration of PGA, Gelofusine, or the combination of the 2 substances. In our mouse model, there was no significant difference in the biodistribution of $[\text{Lys}^{40}(\text{Ahx-DOTA-}^{68}\text{Ga})\text{NH}_2]$ -exendin-4 and $[\text{Lys}^{40}(\text{Ahx-DOTA-}^{111}\text{In})\text{NH}_2]$ -exendin-4. Accordingly, ^{111}In - and ^{68}Ga -labeled exendin-4 may show similar biodistributions and pharmacokinetics in humans. Two small tumors (1.5 and 2.3 mm) in the mouse pancreas were visualized using the same hybrid PET/CT camera as used for patients, showing the high potential of $[\text{Lys}^{40}(\text{Ahx-DOTA-}^{68}\text{Ga})\text{NH}_2]$ -exendin-4 PET in the detection of small tumors. PET has a higher sensitivity and spatial resolution than SPECT (29). This might be important because a high spatial resolution may facilitate the delineation of tumors and kidneys, especially at early time points after injection of the tracer. In a previous clinical study, we showed that the relatively low spatial resolution of $[\text{Lys}^{40}(\text{Ahx-DOTA-}^{111}\text{In})\text{NH}_2]$ -exendin-4 SPECT is a relevant limitation of the method. In 2 of 6 patients, delineation of the tumor from the kidneys was possible only on late scans obtained more than 3 d after injection (20). In addition, a high sensitivity in tumor detection is desirable because 90% of insulinomas are small, with a diameter of less than 2 cm (30). Recent studies using ^{68}Ga -labeled somatostatin receptor agonists showed a high sensitivity in the detection of somatostatin receptor subtype 2-expressing tumors (31–35).

^{68}Ga is a highly suitable positron emitter for PET because it is a generator product with a half-life of 68 min that decays by 89% through positron emission (36). Importantly, the short half-life of ^{68}Ga will cause lower radiation doses to patients than will $[\text{Lys}^{40}(\text{Ahx-DOTA-}^{111}\text{In})\text{NH}_2]$ -exendin-4. In the Rip1Tag2 animal model, $[\text{Lys}^{40}(\text{Ahx-DOTA-}^{68}\text{Ga})\text{NH}_2]$ -exendin-4 showed rapid blood clearance and fast target localization, making short-lived $[\text{Lys}^{40}(\text{Ahx-DOTA-}^{68}\text{Ga})\text{NH}_2]$ -exendin-4 a suitable PET tracer for GLP-1 insulinoma imaging.

Overexpression of GLP-1 receptors not only on insulinoma cells but also on pancreatic β -cells provides a further application of GLP-1 receptor imaging (37–39). Brom et al. evaluated noninvasive β -cell SPECT using the GLP-1 receptor agonist ^{111}In -DTPA-exendin-3. They found a sig-

nificant correlation between ^{111}In -DTPA-exendin-3 uptake and β -cell mass in rats (40). GLP-1 receptor imaging is a noninvasive method with the potential to monitor the β -cell mass during the course of diabetes development and during antidiabetic treatment. Furthermore, the method might be used for noninvasive monitoring of islet cell graft survival after transplantation.

SPECT or SPECT/CT with $^{99\text{m}}\text{Tc}$ -labeled exendin-4 is an alternative approach to GLP-1 receptor imaging with ^{111}In . The estimated effective dose of $[\text{Lys}^{40}(\text{Ahx-HYNIC-}^{99\text{m}}\text{Tc/EDDA})\text{NH}_2]$ -exendin-4 is more than 40 times less than that of its ^{111}In -labeled congener compound because of the low energy and short physical half-life of $^{99\text{m}}\text{Tc}$ and the significantly lower tumor and organ uptake of $[\text{Lys}^{40}(\text{Ahx-HYNIC-}^{99\text{m}}\text{Tc/EDDA})\text{NH}_2]$ -exendin-4, compared with $[\text{Lys}^{40}(\text{Ahx-DOTA-}^{111}\text{In})\text{NH}_2]$ -exendin-4. These data can be explained by the significantly less efficient internalization. Regression analysis showed a significant correlation between the rate of internalization and the uptake in the tumor at 4 h after injection of the respective radiopeptide (Fig. 4). Despite lower tumor uptake, $[\text{Lys}^{40}(\text{Ahx-HYNIC-}^{99\text{m}}\text{Tc/EDDA})\text{NH}_2]$ -exendin-4 multipinhole SPECT detected multiple small tumors (diameter, 1.0–3.2 mm) in the pancreas and is therefore a promising candidate for clinical GLP-1 receptor imaging studies.

In addition, $^{99\text{m}}\text{Tc}$ is a radionuclide suitable for detection with a γ -probe. Hence, intraoperative localization of insulinomas using a normal or endoscopic γ -probe might be an additional clinical application of $[\text{Lys}^{40}(\text{Ahx-HYNIC-}^{99\text{m}}\text{Tc/EDDA})\text{NH}_2]$ -exendin-4.

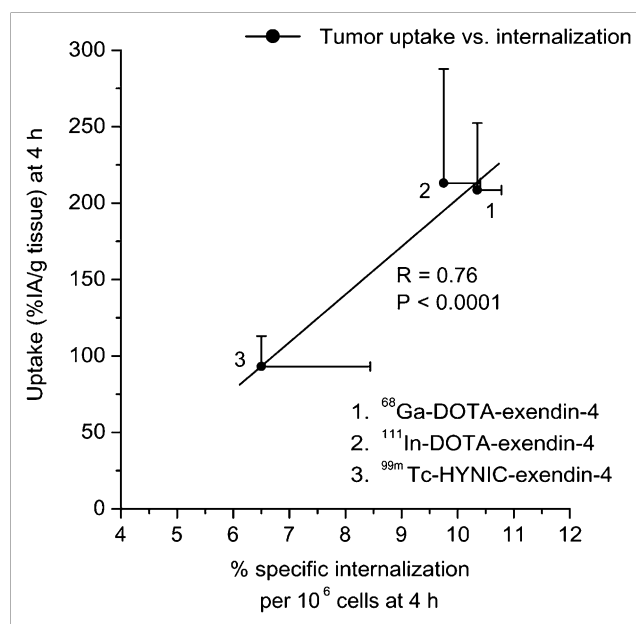


FIGURE 4. Correlation of tumor uptake (%IA/g of tissue) and internalization (percentage of specific internalized/ 10^6 cells) at 4 h. Each data point shows mean tumor uptake \pm SD and mean internalization \pm SD.

CONCLUSION

These promising pharmacokinetic and imaging data show that [Lys⁴⁰(Ahx-DOTA-⁶⁸Ga)NH₂]-exendin-4 and [Lys⁴⁰(Ahx-HYNIC-^{99m}Tc/EDDA)NH₂]-exendin-4 are suitable candidates for clinical GLP-1 receptor imaging studies. PET/CT with [Lys⁴⁰(Ahx-DOTA-⁶⁸Ga)NH₂]-exendin-4 will possibly localize small insulinomas at early time points after injection, and SPECT/CT with [Lys⁴⁰(Ahx-HYNIC-^{99m}Tc/EDDA)NH₂]-exendin-4 will potentially increase the availability of the method.

ACKNOWLEDGMENTS

We thank Novartis Pharma for analytical assistance and Dr. Daniel Storch, Dr. Andreas Baumann, Dr. Stefan Kneifel, Sybille Tschumi, Edith Rauber, and Roland Jost for their expert technical help. During the review process of this manuscript, a paper was published by Brom et al. (41) on the ⁶⁸Ga labeling of a similar peptide showing promising results in a tumor xenograft model. This work was supported in part by Oncosuisse grant OCS-01778-08-2005, grants from the Novartis Foundation and Swiss National Science Foundation (PASMP3-123269, 320000-118333, and COST D38), and a grant from the Yde Foundation.

REFERENCES

1. Reubi JC. Peptide receptors as molecular targets for cancer diagnosis and therapy. *Endocr Rev*. 2003;24:389–427.
2. Schottelius M, Wester HJ. Molecular imaging targeting peptide receptors. *Methods*. 2009;48:161–177.
3. Ricke J, Klose KJ, Mignon M, Oberg K, Wiedenmann B. Standardisation of imaging in neuroendocrine tumours: results of a European delphi process. *Eur J Radiol*. 2001;37:8–17.
4. Krenning EP, Kwekkeboom DJ, Bakker WH, et al. Somatostatin receptor scintigraphy with [¹¹¹In-DTPA-D-Phe¹]- and [¹²³I-Tyr³]-octreotide: the Rotterdam experience with more than 1000 patients. *Eur J Nucl Med*. 1993;20:716–731.
5. Lebtahi R, Cadiot G, Sarda L, et al. Clinical impact of somatostatin receptor scintigraphy in the management of patients with neuroendocrine gastroenteropancreatic tumors. *J Nucl Med*. 1997;38:853–858.
6. Modlin IM, Tang LH. Approaches to the diagnosis of gut neuroendocrine tumors: the last word (today). *Gastroenterology*. 1997;112:583–590.
7. Zimmer T, Stolzel U, Bader M, et al. Endoscopic ultrasonography and somatostatin receptor scintigraphy in the preoperative localisation of insulinomas and gastrinomas. *Gut*. 1996;39:562–568.
8. Reubi JC, Waser B. Concomitant expression of several peptide receptors in neuroendocrine tumours: molecular basis for in vivo multireceptor tumour targeting. *Eur J Nucl Med Mol Imaging*. 2003;30:781–793.
9. Chatziioannou A, Kehagias D, Mourikis D, et al. Imaging and localization of pancreatic insulinomas. *Clin Imaging*. 2001;25:275–283.
10. Ramage JK, Davies AH, Ardill J, et al. Guidelines for the management of gastroenteropancreatic neuroendocrine (including carcinoid) tumours. *Gut*. 2005;54(suppl 4):iv1–iv16.
11. Kauhanen S, Seppanen M, Minn H, et al. Fluorine-18-L-dihydroxyphenylalanine (¹⁸F-DOPA) positron emission tomography as a tool to localize an insulinoma or β-cell hyperplasia in adult patients. *J Clin Endocrinol Metab*. 2007;92:1237–1244.
12. Tessonnier L, Sebag F, Ghander C, et al. Limited value of ¹⁸F-F-DOPA PET to localize pancreatic insulin-secreting tumors in adults with hyperinsulinemic hypoglycemia. *J Clin Endocrinol Metab*. 2010;95:303–307.
13. Wiesli P, Brandle M, Schmid C, et al. Selective arterial calcium stimulation and hepatic venous sampling in the evaluation of hyperinsulinemic hypoglycemia: potential and limitations. *J Vasc Interv Radiol*. 2004;15:1251–1256.
14. Tucker ON, Crotty PL, Conlon KC. The management of insulinoma. *Br J Surg*. 2006;93:264–275.

15. Gotthardt M, Fischer M, Naeher I, et al. Use of the incretin hormone glucagon-like peptide-1 (GLP-1) for the detection of insulinomas: initial experimental results. *Eur J Nucl Med Mol Imaging*. 2002;29:597–606.
16. Gotthardt M, Lalyko G, van Eerd-Vismale J, et al. A new technique for in vivo imaging of specific GLP-1 binding sites: first results in small rodents. *Regul Pept*. 2006;137:162–167.
17. Wild D, Behe M, Wicki A, et al. [Lys⁴⁰(Ahx-DTPA-¹¹¹In)NH₂]-exendin-4, a very promising ligand for glucagon-like peptide-1 (GLP-1) receptor targeting. *J Nucl Med*. 2006;47:2025–2033.
18. Wicki A, Wild D, Storch D, et al. [Lys⁴⁰(Ahx-DTPA-¹¹¹In)NH₂]-Exendin-4 is a highly efficient radiotherapeutic for glucagon-like peptide-1 receptor-targeted therapy for insulinoma. *Clin Cancer Res*. 2007;13:3696–3705.
19. Wild D, Macke H, Christ E, Gloor B, Reubi JC. Glucagon-like peptide 1-receptor scans to localize occult insulinomas. *N Engl J Med*. 2008;359:766–768.
20. Christ E, Wild D, Forrer F, et al. Glucagon-like peptide-1 receptor imaging for localization of insulinomas. *J Clin Endocrinol Metab*. 2009;94:4398–4405.
21. IUPAC-IUB Commission on Biochemical Nomenclature (CBN). Symbols for amino-acid derivatives and peptides, recommendations 1971. *Eur J Biochem*. 1972;27:201–207.
22. Schramm NU, Ebel G, Engeland U, Schurrat T, Behe M, Behr TM. High-resolution SPECT using multi-pinhole collimation. *IEEE Trans Nucl Sci*. 2003;50:315–320.
23. Stabin MG, Sparks RB, Crowe E. OLINDA/EXM: the second-generation personal computer software for internal dose assessment in nuclear medicine. *J Nucl Med*. 2005;46:1023–1027.
24. Zernosekov KP, Filosofov DV, Baum RP, et al. Processing of generator-produced ⁶⁸Ga for medical application. *J Nucl Med*. 2007;48:1741–1748.
25. Hanahan D. Heritable formation of pancreatic beta-cell tumours in transgenic mice expressing recombinant insulin/simian virus 40 oncogenes. *Nature*. 1985;315:115–122.
26. Sgouros G. Bone marrow dosimetry for radioimmunotherapy: theoretical considerations. *J Nucl Med*. 1993;34:689–694.
27. International Commission on Radiological Protection (ICRP). *Recommendations of the International Commission on Radiological Protection*. ICRP publication 60. Oxford, U.K.: Pergamon Press; 1991.
28. Gotthardt M, van Eerd-Vismale J, Oyen WJ, et al. Indication for different mechanisms of kidney uptake of radiolabeled peptides. *J Nucl Med*. 2007;48:596–601.
29. Martin WH, Delbecke D, Patton JA, Sandler MP. Detection of malignancies with SPECT versus PET, with 2-[fluorine-18]fluoro-2-deoxy-D-glucose. *Radiology*. 1996;198:225–231.
30. Gouya H, Vignaux O, Augui J, et al. CT, endoscopic sonography, and a combined protocol for preoperative evaluation of pancreatic insulinomas. *AJR*. 2003;181:987–992.
31. Antunes P, Ginj M, Zhang H, et al. Are radiogallium-labelled DOTA-conjugated somatostatin analogues superior to those labelled with other radiometals? *Eur J Nucl Med Mol Imaging*. 2007;34:982–993.
32. Gabriel M, Decristoforo C, Kandler D, et al. ⁶⁸Ga-DOTA-Tyr³-octreotide PET in neuroendocrine tumors: comparison with somatostatin receptor scintigraphy and CT. *J Nucl Med*. 2007;48:508–518.
33. Kayani I, Bomanji JB, Groves A, et al. Functional imaging of neuroendocrine tumors with combined PET/CT using ⁶⁸Ga-DOTATATE (DOTA-DPhe¹, Tyr³-octreotate) and ¹⁸F-FDG. *Cancer*. 2008;112:2447–2455.
34. Ambrosini V, Tomassetti P, Castellucci P, et al. Comparison between ⁶⁸Ga-DOTA-NOC and ¹⁸F-DOPA PET for the detection of gastro-entero-pancreatic and lung neuro-endocrine tumours. *Eur J Nucl Med Mol Imaging*. 2008;35:1431–1438.
35. Buchmann I, Henze M, Engelbrecht S, et al. Comparison of ⁶⁸Ga-DOTATOC PET and ¹¹¹In-DTPAOC (Octreoscan) SPECT in patients with neuroendocrine tumours. *Eur J Nucl Med Mol Imaging*. 2007;34:1617–1626.
36. Maecke HR, Hofmann M, Haberkorn U. ⁶⁸Ga-labeled peptides in tumor imaging. *J Nucl Med*. 2005;46(suppl 1):172S–178S.
37. Kieffer TJ, Habener JF. The glucagon-like peptides. *Endocr Rev*. 1999;20:876–913.
38. Korner M, Stockli M, Waser B, Reubi JC. GLP-1 receptor expression in human tumors and human normal tissues: potential for in vivo targeting. *J Nucl Med*. 2007;48:736–743.
39. Tornehave D, Kristensen P, Romer J, Knudsen LB, Heller RS. Expression of the GLP-1 receptor in mouse, rat, and human pancreas. *J Histochem Cytochem*. 2008;56:841–851.
40. Brom M, Baumeister P, Melis M, et al. Determination of the β-cell mass by SPECT imaging with In-111-DTPA-exendin-3 in rats [abstract]. *J Nucl Med*. 2009;50(suppl 2):147.
41. Brom M, Oyen WJ, Joosten L, Gotthardt M, Boerman OC. ⁶⁸Ga-labelled exendin-3, a new agent for the detection of insulinomas with PET. *Eur J Nucl Med Mol Imaging*. January 29, 2010 [Epub ahead of print].